HIGHER-ORDER MOMENT MODELS OF LONGITUDINAL PULSE SHAPE EVOLUTION IN PHOTOINJECTORS*

C. Mitchell†, J. Qiang, F. Sannibale, M. Venturini, C. Papadopoulos, D. Filippetto, H. Qian, R. Huang
LBNL, Berkeley, CA 94720, USA

Abstract

The presence of longitudinal asymmetry, sometimes in the form of a one-sided tail, in the current profile emerging from low-energy photoinjectors can strongly impact the beam quality downstream of the compression region of an FEL beam delivery system. To understand the origin of this feature, an approximate model for the evolution of higher-order longitudinal beam moments is developed in the presence of nonlinear kinematic effects and longitudinal space-charge. This model is applied to investigate the evolution of beam skewness in injector systems with parameters similar to the APEX Injector under investigation at Lawrence Berkeley National Laboratory.

INTRODUCTION

Careful control of the longitudinal phase space distribution of each electron bunch exiting an FEL beam delivery system is critical to optimizing the FEL radiation brightness and coherence. Previous studies have shown that, in some cases, an asymmetric tail may appear in the beam current profile out of the injector [1], limiting the portion of charge that contributes to the lasing process. To understand this feature, we attempted to develop a simple model of the longitudinal pulse shape evolution in low-energy photoinjectors using a moment description.

The utility of the second-order rms beam envelope equations [2] has led to the study of systems of such equations for higher-order beam moments [3,4]. Our approach is based on the Hamiltonian formulation of the Vlasov-Poisson equation as described in [5], which provides a systematic framework for constructing moment equations through a given order [6]. The resulting system of equations describes the longitudinal beam moments through fourth order, using a 1D wakefield model of the longitudinal space-charge interaction.

This model was applied to an LCLS-II type injector system based on the design of the Advanced Photoinjector Experiment (APEX) at Lawrence Berkeley National Laboratory [7], whose layout is shown in Fig. 1. After photoemission from a 186 MHz RF gun, each bunch passes through a 1.3 GHz buncher cavity operated near 90° off-crest, which introduces an energy-bunch length correlation. The bunch then undergoes ballistic compression in a drift before entering the first of several 9-cell 1.3 GHz TESLA accelerating cavities.

In the following section, we characterize the longitudinal pulse shape in the injector using a moment description. In the remainder of the paper, this characterization is used to investigate the origin and evolution of longitudinal beam asymmetry in the presence of ballistic compression.

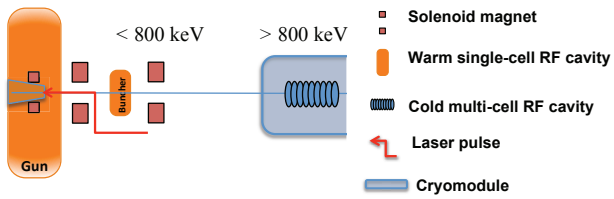

Figure 1: The low-energy portion of the photoinjector for an FEL beam delivery system based on the APEX design.

PULSE SHAPE CHARACTERIZATION

It is useful to characterize the shape of the electron bunch current profile in terms of the sequence of standardized moments:

$$\mu_n = \left\langle \left(\frac{z - \langle z \rangle}{\sigma_z} \right)^n \right\rangle, \quad n = 0, 1, 2, \ldots, \tag{1}$$

where z denotes the longitudinal coordinate within the bunch and σ_z the rms bunch length. The quantities μ_3 and μ_4 define the beam skewness and kurtosis, respectively, which must satisfy the inequality [8]:

$$\mu_4 \geq \mu_3^2 + 1. \tag{2}$$

The skewness is a measure of bunch asymmetry: for a bunch with a unimodal density profile, a value $\mu_3 > 0$ denotes that a low-density tail appears for $z > \langle z \rangle$, while $\mu_3 < 0$ denotes that a low-density tail appears for $z < \langle z \rangle$. The kurtosis is often described as a measure of "peakedness", and for a Gaussian profile takes the value $\mu_4 = 3$. Note that many authors use the excess kurtosis, defined by $\mu_4 - 3$.

An approximation to the shape of the beam current profile can be obtained by matching the centroid location, rms bunch length, and the moments (μ_3, μ_4) to a corresponding probability distribution from the Pearson family [9]- [12]. Figure 2 illustrates the current profile of a 300 pC, 99 MeV electron bunch at the exit of a proposed LCLS-II injector system based on the APEX design (Fig. 1), together with a Pearson distribution of matching skewness and kurtosis. Note the asymmetry of the current profile, with a slight tail appearing for $z < 0$.

Figure 3 illustrates the evolution of the skewness and kurtosis of this bunch during the first 3.5 m of the injector system of Fig. 1 as simulated using IMPACT-T [13]. The beam is nearly symmetric at the exit of the buncher, with

* Work supported by the U.S. Department of Energy under Contract No. DE-AC02-05CH11231.
† ChadMitchell@lbl.gov

ISBN 978-3-95450-133-5

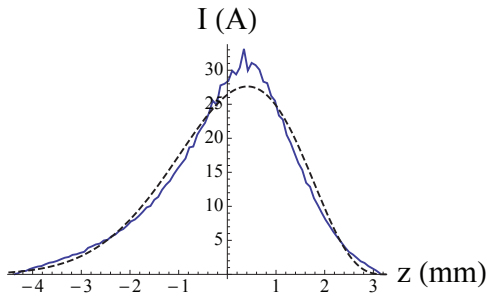

Figure 2: The simulated current profile of a 300 pC, 99 MeV bunch at the exit of a proposed LCLS-II injector (solid) is shown together with a Pearson Type I distribution (dashed) with matched $(\mu_3, \mu_4) = (-0.521, 3.132)$.

$\mu_3 = 0.06$, and the values (μ_3, μ_4) change significantly in the drift region between the buncher exit (1 m) and the pre-booster entrance (2.2 m). These values remain nearly unchanged from 10 cm beyond the pre-booster entrance through the remainder of the acceleration system. As a result, the final pulse shape appears to be set primarily by the dynamics in the ballistic compression region, which will be the focus of this paper.

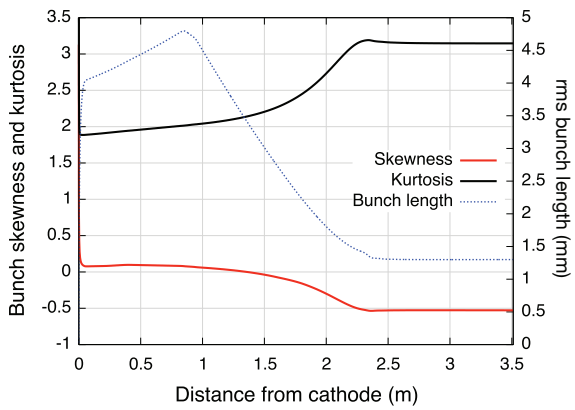

Figure 3: The skewness μ_3, kurtosis μ_4, and bunch length σ_z are shown as a function of bunch centroid distance from the cathode for the layout shown in Fig. 1.

NONLINEAR BALLISTIC COMPRESSION

The Hamiltonian describing longitudinal single-particle motion within a drifting beam relative to a nominal reference particle can be written in terms of the canonical variables $z = -c\Delta t$, $\delta = \Delta\gamma/\gamma$ in the form:

$$H_1(z,\delta) = -\sqrt{(1+\delta)^2 - 1/\gamma^2} + (1+\delta)/\beta, \qquad (3)$$

where

$$\gamma = 1/\sqrt{1-\beta^2} \qquad (4)$$

denotes the nominal relativistic gamma factor, the drift distance s is taken as the independent variable, and Δt, $\Delta\gamma$ denote deviations from the nominal trajectory.

The Taylor map associated with (3) is given through terms of degree 3 by:

$$z = z_i + R_{56}\delta_i + T_{566}\delta_i^2 + U_{5666}\delta_i^3, \qquad \delta = \delta_i \qquad (5)$$

where

$$R_{56}(s) = \frac{s\gamma}{(\gamma^2-1)^{3/2}}, \quad T_{566}(s) = -\frac{3}{2}\frac{s\gamma^3}{(\gamma^2-1)^{5/2}},$$
$$U_{5666}(s) = \frac{1}{2}\frac{s(4\gamma^2+1)\gamma^3}{(\gamma^2-1)^{7/2}}.$$

Consider a beam with a linear relative energy chirp $h = d\delta/dz < 0$ and small uncorrelated energy spread $\sigma_\delta << |h\sigma_z|$ entering a drift region. Using (5), one can obtain the evolution of the standardized moments (1) as functions of the initial moments $\mu_{n,i}$ and the two dimensionless parameters:

$$\alpha = h^2 T_{566}\sigma_{z,i}C, \qquad \beta = h^3 U_{5666}\sigma_{z,i}^2 C, \qquad (6)$$

where $C = 1/(1+hR_{56})$ is the linear compression factor. In the typical case when $|\beta| << |\alpha| << 1$, so that nonlinear effects are moderately weak, we find that:

$$\mu_3 = \mu_{3,i} + 3\alpha(\mu_{4,i} - \mu_{3,i}^2 - 1) + O(\alpha^2). \qquad (7)$$

It follows from (7) and (2) that an initially symmetric beam (with $\mu_{3,i} = 0$) is driven toward values of increasingly negative skewness through the nonlinear effect of nonzero T_{566}.

Eliminating h in favor of the compression factor C gives an approximate expression for the final beam skewness exiting a ballistic compression region of length L in the absence of space-charge:

$$\mu_3 = \mu_{3,i} + \frac{9}{2}\frac{(C-1)^2}{C}\left(\frac{\sigma_{z,i}}{L}\right)(1+\mu_{3,i}^2 - \mu_{4,i})\gamma(\gamma^2-1)^{1/2}. \qquad (8)$$

The development of beam asymmetry in a drift is a relativistic effect that grows with increasing beam energy, as apparent in (8).

A MOMENT MODEL OF LONGITUDINAL SPACE-CHARGE

The 2D relativistic Vlasov equation for a drifting beam takes the form:

$$\frac{\partial f}{\partial s} + \frac{\partial H_1}{\partial \delta}\frac{\partial f}{\partial z} + \frac{qE_z}{mc^2\gamma}\frac{\partial f}{\partial \delta} = 0, \qquad (9)$$

where E_z is the longitudinal space-charge electric field and H_1 is given in (3). Following the formalism of [14]- [15], (9) possesses the Lie-Poisson structure of a continuous Hamiltonian system with the collective Hamiltonian given by:

$$H_{\text{coll}} = \int H_1(\zeta)f(\zeta)d\zeta + \frac{1}{2}\frac{q}{mc^2\gamma}\int \phi(z)f(\zeta)d\zeta, \qquad (10)$$

where $\zeta = (z,\delta)$ and the potential ϕ satisfies:

$$E_z(z) = -\frac{\partial\phi}{\partial z}. \qquad (11)$$

ISBN 978-3-95450-133-5

We use a simple model of the longitudinal space-charge wakefield, given in terms of the line-charge density ρ by [16, 17]:

$$E_z(z) = -\frac{g}{4\pi\epsilon_0\gamma^2}\rho'(z), \quad \phi(z) = \frac{g}{4\pi\epsilon_0\gamma^2}\rho(z), \quad (12)$$

where g is a geometrical factor that depends on the boundary conditions. Writing

$$\rho(z) = qN_b\lambda(z), \quad \lambda(z) = \int f(z,\delta)d\delta, \quad (13)$$

where N_b is the number of particles in the bunch and λ is a probability density describing the longitudinal profile of the beam, the second term in (10) then takes the form:

$$H_{\rm int} = \frac{g}{2}\frac{N_b r_c}{\gamma^3}\int \lambda(z)^2 dz, \quad (14)$$

where r_c is the classical electron radius.

Given any basis of polynomials $\{P_\alpha : \alpha = 1,2,\ldots,n\}$ of degree 1-N in the phase-space variables $\zeta = (z,\delta)$, we define a set of moments associated with the distribution function f by:

$$m_\alpha = \int P_\alpha(\zeta) f(\zeta) d\zeta \quad (\alpha = 1,2,\ldots,n). \quad (15)$$

If $H_{\rm coll}$ can be expressed as a function of the moments m_α, then the system of equations for the moments through order N takes the form [6]:

$$\frac{dm_\alpha}{ds} = \sum_{\beta=1}^{n} \frac{\partial H_{\rm coll}}{\partial m_\beta}\langle\{P_\alpha, P_\beta\}\rangle, \quad (16)$$

where $\{,\}$ denotes the usual Poisson bracket.

Working through order $N = 4$, there are 14 such equations. The single-particle term in (10) is expressed as a function of the moments m_α by expanding H_1 as a Taylor series of degree 4. The interaction term $H_{\rm int}$ is expressed as a function of the moments by evaluating (14) when λ is taken to be the unique Pearson distribution that has the specified moments through fourth order [11]. This allows (14) to be written in the form:

$$H_{\rm int} = \frac{g}{2}\frac{N_b r_c}{\gamma^3\sigma_z}\tilde{H}_{\rm int}(\mu_3,\mu_4), \quad (17)$$

where $\tilde{H}_{\rm int}$ is a function of the beam skewness and kurtosis only. Figure 4 shows the contours of $\tilde{H}_{\rm int}$, indicating a global minimum at $(\mu_3,\mu_4) = (0, 2.14286)$, which corresponds to a parabolic current profile.

As is typical of the hierarchy of moment equations [3], the system (16) couples the desired set of moments (through order 4) to moments of higher order (through order 6). We close the system by substituting analytical expressions for the 5-6th order moments that are obtained in the absence of space-charge using the single-particle map (5). This procedure is expected to introduce significant error when the effects of space-charge are sufficiently large.

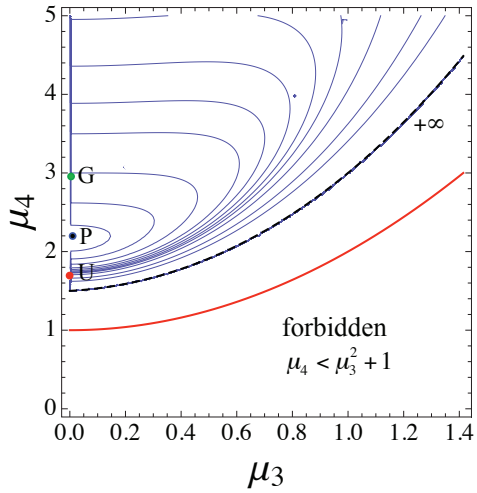

Figure 4: Contours of the space-charge interaction Hamiltonian (17) in the Pearson plane, showing the locations corresponding to Gaussian (G), parabolic (P), and uniform (U) current profiles. The quantity $\tilde{H}_{\rm int}$ is minimum for a parabolic profile and diverges along the solid black curve. The figure is symmetric about the line $\mu_3 = 0$.

APPLICATION

The moment model of the previous section was used together with the code IMPACT-Z to investigate the evolution of beam skewness and kurtosis in the ballistic compression region of an APEX-type photoinjector (Fig. 1). For each simulation, a bunch with an initially symmetric current profile and a linear energy chirp (at the buncher exit) was modeled during its 1.2 m drift between the buncher and the entrance of the first accelerating cavity. In order to study the beam longitudinal dynamics using IMPACT's 3D Poisson solver, only the longitudinal component of the space-charge electric field is included. In each case, the initial rms bunch length is fixed at 4.36 mm and the initial energy chirp of the beam is adjusted to produce a compression factor of 3.

Figure 5 shows the trajectory of a bunch in the plane (μ_3,μ_4) at a kinetic energy of 821 keV for several values of bunch charge. The initial longitudinal current profile is Gaussian, corresponding to $(\mu_3,\mu_4) = (0,3)$. In the absence of space-charge, the magnitude of both the skewness and kurtosis increase along the drift, with the final skewness given correctly by (8). The effect of space-charge appears to be to drive the skewness and kurtosis values toward those of a parabolic profile, consistent with minimizing the interaction energy shown in Fig. 4.

Figure 6 shows the beam skewness at the exit of the drift as a function of the beam kinetic energy for a fixed bunch charge of 300 pC. Results are shown for a bunch with an initially Gaussian longitudinal profile and for an initially parabolic longitudinal profile. As is predicted in the absence of space-charge (8), the skewness increases with the beam energy. Note that the final skewness depends significantly on the details of the initial longitudinal profile of the beam.

ISBN 978-3-95450-133-5

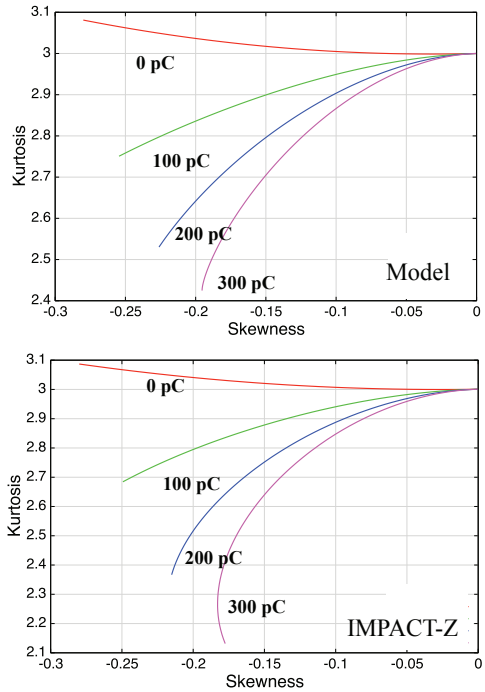

Figure 5: Beam skewness and kurtosis evolution predicted by the moment model (16) (upper) and by IMPACT-Z (lower) for an initially Gaussian 821 keV beam undergoing ballistic compression by a factor of 3 over a 1.2 m drift.

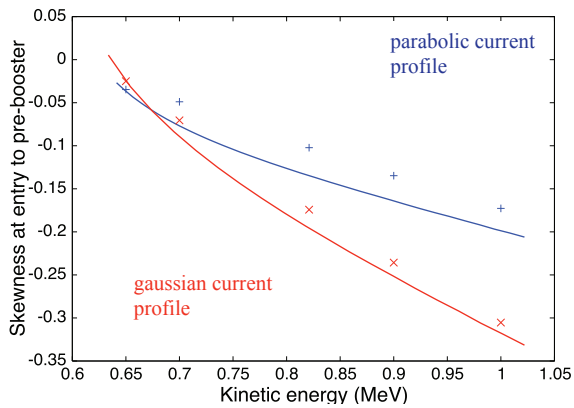

Figure 6: Final beam skewness as a function of beam energy at the exit of 1.2 m drift. Curves are results from the moment model (16), while points are taken from IMPACT-Z simulation.

CONCLUSIONS

A fourth-order moment model was developed for modeling longitudinal beam dynamics in the ballistic compression region of an FEL photoinjector, using a simple model of the longitudinal space-charge wakefield (12). The model predicts scaling of the final beam skewness with the bunch charge and beam energy that is consistent with simulation in IMPACT-Z in the presence of 1D space-charge. The transverse dynamics of the beam are not considered here. In particular, the transverse beam size appears only through the factor g governing the strength of the space-charge wakefield, which is held fixed for these studies.

It is expected that a more accurate model could be obtained by replacing the wakefield (12) by the wakefield obtained from an appropriate longitudinal space-charge impedance [18]. Alternative schemes for closing the set of moment equations are also under consideration.

ACKNOWLEDGEMENT

This work is supported by the Office of Science of the U.S. Department of Energy under Contract No. DE-AC02-05CH11231 and made use of computer resources at the National Energy Research Scientific Computing Center.

REFERENCES

[1] C. Papadopoulos *et al.*, "Injector Design Studies for NGLS", FEL'13, New York, August 2013, TUPSO69 (2013), http://www.JACoW.org

[2] F. J. Sacherer, IEEE Trans. Nucl. Sci. NS-18, 1105 (1971).

[3] P. J. Channell, IEEE Trans. Nucl. Sci. NS-30, 2607 (1983).

[4] W. P. Lysenko, AIP Conf. Proc. 297, 516 (1993).

[5] P. J. Morrison, Phys. Lett. 80A, 383 (1980).

[6] B. A. Shadwick and J. S. Wurtele, "General Moment Model of Beam Transport", PAC'99, New York, March 1999, 2888 (1999), http://www.JACoW.org

[7] F. Sannibale *et al.*, Phys. Rev. ST Accel. Beams 15, 103501 (2012).

[8] V. K. Rohatgi and G. J. Székeley, Stat. and Prob. Lett. 8, 297 (1989).

[9] K. Pearson, Phil. Trans. Royal Soc. London A 216, 429 (1916).

[10] C. C. Craig, Annals Math. Stat. 7, 16 (1936).

[11] A. Stuart and J. K. Ord, *Kendall's Advanced Theory of Statistics*, vol. 1, 6th ed., (Oxford: Oxford University Press, 1994), 215.

[12] H. Jeffreys, *Theory of Probability*, 3rd ed., (Oxford: Oxford University Press, 1961), 74.

[13] J. Qiang, S. Lidia, and R. Ryne, Phys. Rev. ST - Accel. Beams 9, 044204 (2006).

[14] J. E. Marsden and A. Weinstein, Physica 4D, 394 (1982).

[15] I. Bialynicki-Birula and J. C. Hubbard, Physica 128A, 509 (1984).

[16] M. Reiser, *Theory and Design of Charged Particle Beams*, 2nd ed., (Weinheim: Wiley-VCH, 2008), 398.

[17] A. Chao, *Physics of Collective Instabilities in High Energy Accelerators*, (New York: John Wiley, 1993), 23.

[18] M. Venturini, Phys. Rev. ST Accel. Beams 11, 034401 (2008).

ISBN 978-3-95450-133-5